Original Research

Oral ellagic acid attenuated LPS-induced neuroinflammation in rat brain: MEK1 interaction and M2 microglial polarization

Yu-Ling Liu[1], Hui-Ju Huang[2], Sheh-Yi Sheu[3,4], Yu-Cheng Liu[3], I-Jung Lee[5], Shao-Chin Chiang[6,7] and Anya Maan-Yuh Lin[2,6]

[1]Department of Pharmacology, National Yang Ming Chiao Tung University, Taipei 112; [2]Department of Medical Research, Taipei Veterans General Hospital, Taipei 112; [3]Institute of Biomedical Informatics, National Yang Ming Chiao Tung University, Taipei 112; [4]Department of Life Sciences and Institute of Genome Sciences, National Yang Ming Chiao Tung University, Taipei 112; [5]Pharmaceutical Botany Research Laboratory, Yokohama University of Pharmacy, Yokohama 245-0066, Japan; [6]Department of Pharmacy, National Yang Ming Chiao Tung University, Taipei 112; [7]Department of Pharmacy, Koo Foundation Sun Yat-Sen Cancer center, Taipei, Taiwan
Corresponding authors: Shao-Chin Chiang. Email: scchiang316@nycu.edu.tw; Anya Maan-Yuh Lin. Emails: myalin@nycu.edu.tw; myalin@vghtpe.gov.tw

Impact Statement

To evaluate the neurotherapeutic activity of ellagic acid, the cellular mechanism underlying ellagic acid–induced neuroprotection is elucidated. Using *in silico* assay and selumetinib, we characterize the involvement of MEK1–ERK signaling in ellagic acid–induced neuroprotection. Our *in vivo* study suggests that oral administration of ellagic acid is neuroprotective via inhibiting MEK1–ERK signaling to inhibit lipopolysaccharide (LPS)-induced neuroinflammation in the rat brain. Furthermore, we investigate the M2 polarization is one of the protective mechanisms responsible for ellagic acid–induced inhibition of LPS-induced neuroinflammation, indicating that M1/M2 transition may be used as a druggable target for treating central nervous system (CNS) neurodegenerative diseases.

Abstract

Ellagic acid, the marker component of peels of *Punica granatum* L., is known traditionally to treat traumatic hemorrhage. In this study, the cellular mechanism underlying ellagic acid-induced anti-inflammation was investigated using lipopolysaccharides (LPSs) as a neuroinflammation inducer. Our *in vitro* data showed that LPS (1 μg/mL) consistently phosphorylated ERK and induced neuroinflammation, such as elevation in tumor necrosis factor-α (TNF-α) and nitric oxide production in treated BV-2 cells. Incubation of ellagic acid significantly inhibited LPS-induced ERK phosphorylation and subsequent neuroinflammation in treated BV-2 cells. Furthermore, our *in vivo* study of neuroinflammation employed an intranigral infusion of LPS that resulted in a time-dependent elevation in phosphorylated ERK levels in the infused substantia nigra (SN). Oral administration of ellagic acid (100 mg/kg) significantly attenuated LPS-induced ERK phosphorylation. A four-day treatment of ellagic acid did not alter LPS-induced ED-1 elevation but ameliorated LPS-induced reduction in CD206 and arginase-1 (two biomarkers of M2 microglia). A seven-day treatment of ellagic acid abolished LPS-induced increases in heme-oxygenase-1, cyclo-oxygenase 2, and α-synuclein trimer levels (a pathological hallmark) in the infused SN. At the same time, ellagic acid attenuated LPS-induced increases in active caspase 3 and receptor-interacting protein kinase-3 levels (respective biomarkers of apoptosis and necroptosis) as well as reduction in tyrosine hydroxylase–positive cells in the infused SN. *In silico* analysis showed that ellagic acid binds to the catalytic site of MEK1. Our data suggest that ellagic acid is capable of inhibiting MEK1–ERK signaling and then attenuated LPS-induced neuroinflammation, protein aggregation, and programmed cell deaths. Moreover, M2 microglial polarization is suggested as a novel antineuroinflammatory mechanism in the ellagic acid–induced neuroprotection.

Keywords: Ellagic acid, MEK-1, selumetinib, *in silico* assay, neuroinflammation, M2 microglial polarization

***Experimental Biology and Medicine* 2023; 248: 656–664. DOI: 10.1177/15353702231182230**

Introduction

Clinically, activated microglia, the primary brain cells responsible for neuroinflammation, was detected in the brain of patients with Parkinson's disease (PD), Alzheimer's disease, and traumatic brain injury, indicating a pathological role of activated microglia in the central nervous system (CNS) neurodegenerative diseases.[1–3] In response to insults, resting microglia become activated and amoeboid to migrate and phagocytose as well as produce cytokines which affect near-by neurons and astrocytes.[4] To support this notion, several neurotoxins, including 1-methyl-4-phenylpyridinium[5,6] and acrolein, have been employed to induce neuroinflammation in rat brain, including activation of glial cells, increases in proinflammatory enzymes, and oxidative injury.[7] Moreover, a significant body of studies

has shown that ablation of neuroinflammation is capable of attenuating neurotoxicity,[5,7–12] suggesting that inhibiting neuroinflammation is a therapeutic strategy for treating CNS neurodegenerative diseases.[13]

During the neuroinflammation, two phenotypic types of activated microglia are identified.[14,15] One is the classical "M1" microglia that is proinflammatory by releasing proinflammatory cytokines, generating high reactive oxygen species (ROS) and becoming phagocytic. The other is "M2" microglia that is anti-inflammatory by releasing anti-inflammatory cytokines and low levels of ROS.[14,15] An imbalanced M1/M2 transition, such as excessive activation of M1 microglia[14] and/or reduced function of M2 microglia, is suggested in the pathophysiology of neuroinflammation.[16] To support of this notion, lipopolysaccharide (LPS), a bacterial endotoxin is commonly used to induce neuroinflammation[17–19] and modulate microglial polarization.[20,21] Our previous study showed intranigral infusion of LPS elevated iNOS (M1 biomarker) in the LPS-treated substantia nigra (SN).[9] Furthermore, many studies have demonstrated neuroprotective effects by inhibiting M1 polarization.[9,22] Therefore, microglial transition toward a beneficial M2 condition appears to be a druggable target in treating CNS neurodegenerative diseases.[23]

To search potential therapeutic strategies against neuroinflammation, we focused on the neuroprotective effect of ellagic acid, the marker component of *Punica granatum* L., which is a Chinese traditional medicine known for treating traumatic hemorrhage.[24] Many *in vitro* studies have reported the neuroprotective effects of ellagic acid on glial cells and neurons, including suppression of tumor necrosis factor-α (TNF-α) secretion in glia as well as reduction in α-synuclein aggregation and toxic Aβ fragments formation in neurons.[25,26] Similarly, animal studies have demonstrated that ellagic acid attenuated behavioral deficits by Aβ[8] and cerebral ischemia by permanent middle cerebral artery occlusion[10] as well as neuroinflammation and neurodegeneration by 6-hydroxydopamine (6-OHDA).[27,28] In contrast to the mounting studies on ellagic acid–induced antioxidative and anti-inflammatory responses,[10,26] limited studies have focused on the microglial transition in ellagic acid–induced neuroprotection.

After binding to toll-like receptors (TLRs),[29] LPS is known to activate several cellular signalings, including MAPK[30] and PI3K–AKT pathways.[12] We further demonstrated that selumetinib (AZD 6244), an MEK–ERK inhibitor for cancer therapy, blocked LPS-induced ERK phosphorylation and neuroinflammation, indicating that LPS induced neuroinflammation via activating MEK–ERK signaling pathway.[31] In this study, we employed LPS to establish neuroinflammation *in vitro* and *in vivo*. The aim was two-fold. One was to investigate the involvement of MEK–ERK signaling pathway in ellagic acid–induced neuroprotection. *In silico* analysis using molecular docking technique was employed to further demonstrate the interaction of ellagic acid and MEK-1. The other was to delineate the ellagic acid–induced inhibition of LPS-induced neuroinflammation, including M1/M2 microglial transition[30] and subsequent programmed cell death.

Materials and methods

Drugs

The chemicals used were ellagic acid (Sigma, St. Louis, MO, USA), LPS (Sigma), dimethyl sulfoxide (DMSO, Sigma) as a vehicle for *in vitro* study and methylcellulose (Sigma) as an excipient for *in vivo* study.

Cultures of BV-2 cells

The BV-2 cells line was established from microglial cells of C57BL/6 mouse brain and was maintained in Dulbecco's Modified Eagle Medium supplemented with 10% (v/v) fetal bovine serum and 1% penicillin-streptomycin-amphotericin B in an incubator under 5% CO_2 at 37°C.

NO measurement

At the end of experiment, the culture medium was collected for measuring NO production by BV-2 cells. The culture medium was mixed with an equal volume of the Griess reagent (1% sulfanilamide, 0.1% *N*-(1-Naphthyl)ethylenediamine in 2.5% H_2PO_4) and incubated for 15 min at room temperature in the dark. Nitrite concentration was determined by measuring the absorbance at 550 nm using an ELISA plate reader (TECAN Sunrise, Männedorf, Switzerland).

Animals

Adult, male Sprague-Dawley (SD) rats, weighing 300–350 g, were supplied by BioLASCO Taiwan Co., Ltd. (Yilan, Taiwan). All animals (three rats/individually ventilated cage) were housed in an air-conditioned room (22 ± 2°C) on a 12 h light/dark cycle (07:00–19:00 h light) and had free access to food and water. The use of animals has been approved by the Institutional Animal Care and Use Committee of Taipei Veterans General Hospital, Taipei, Taiwan, R.O.C. The approval number is IACUC2018-186. All experiments were performed in the accordance with relevant guidelines and regulation.

Intranigral infusion of drug

Adult, male SD rats were anesthetized with pentobarbital (50–60 mg/kg, intraperitoneal, Sigma) and immobilized in a stereotaxic instrument (David Kopf Instruments, Palo Alto, CA, USA). The skin was incised to expose the parietal bone, one hole was drilled above the cortical surface for local infusion of LPS (4 μg/μL) unilaterally in the SN with coordinates of 3.2 mm anterior, 2 mm above the interaural zero, 2.1 mm lateral to the midline, and 3.5 mm below the incisor bar. One microliter saline solution containing 4 μg LPS was infused at a rate of 0.2 μL/min through a stainless steel needle (30-gauge). After the infusion, the stainless steel needle was held in place for an additional 5 min. After the surgery, rats recovered from anesthesia and were placed in home cages for the indicated times.

Oral administration of ellagic acid

Rats were randomly divided in two groups. The control group received methylcellulose (0.5%) as vehicle and the

other group received ellagic acid (100 mg/kg in 0.5% methylcellulose) using an oral gavage needle 1 h prior to an intranigral infusion of LPS. Afterwards, daily administration of ellagic acid continued as indicated for each experiment.

Western blot analysis of relevant proteins

At the end of *in vitro* study, cells were treated with a radioimmunoprecipitation assay (RIPA) buffer containing ethylenediaminetetraacetic acid-Na (1 mM), NaCl (0.5 M), Tris (50 mM), sodium dodecyl sulfate (SDS, 0.05%), phenylmethanesulphonyl fluoride (1 mM), and Triton X-100 (0.5%). The lysates of cultured cells were centrifuged at 4°C, 16,500*g* for 0.5 h. The supernatant was stored at −80°C for further analysis. At the end of *in vivo* study, dissected rat SN was homogenized in protease inhibitor cocktail (40 μL) (Calbiochem, San Diego, CA, USA) at 0°C. The cell lysates were centrifuged at 15,000*g* for 30 min at 4°C, and the supernatant was stored at −80°C.

For western blot assay, 30 μg protein samples were run on 8–12% SDS-polyacrylamide gel electrophoresis. Afterwards, protein samples on the gel were transferred onto a nitrocellulose membrane (Bio-Rad, Hercules, CA, USA) at 80 V for 2 h. Protein blots were probed with a monoclonal antibody against p-ERK, total ERK (Cell Signaling Tech., Beverly, MA, USA), TNF-α, ED-1 (Bio-Rad Laboratories, Inc., Hercules, CA, USA), CD206 (Cell Signaling Tech.), arginase 1 (Cell Signaling Tech.), HO-1 (Enzo Life Sciences, Farmingdale, NY, USA), cyclo-oxygenase 2 (COX-2), α-synuclein (Cell Signaling Tech.), procaspase 3/cleaved caspase 3, and RIPK3 (Cell Signaling Tech.) at room temperature for 2 h. Horseradish peroxidase–conjugated secondary immunoglobulin G (IgG) (Chemicon, Temecula, CA, USA) was used as a secondary antibody for western blot assay. The immunoreaction was visualized by the Amersham-enhanced chemiluminescence (Amersham Pharmacia Biotech, Piscataway, NJ, USA). After this detection, the bound primary and secondary antibodies were stripped by incubating the membrane in stripping buffer (100 mM 2-mercaptoethanol, 2% SDS) at 50°C for 45 min. The membrane was reprobed with a mouse β-actin antibody (Millipore, Burlington, MA, USA). The densities of blots were analyzed using a scanning densitometer that was operated by Scanner Control software (Molecular Dynamics, Sunnyvale, CA, USA). Results were obtained by calculating the density using Imagequant software (American Biosciences, Pittsburgh, PA, USA) and reported as relative optical density of the specific proteins.

Immunofluorescence staining of tyrosine hydroxylase

At the end of *in vivo* study, rats were transcardially perfused with 0.9% saline followed by a fixative consisting of paraformaldehyde (4%) in 0.1 M phosphate-buffered saline (PBS). Brains were removed and immersed in 30% sucrose buffer solution overnight and then sectioned coronally at 30 μm thickness using a cryostat (Leica CM 1950, Wetzlar, Germany). Brain sections were washed with PBS, incubated with Triton X-100 (0.3%) and goat serum (1% GS; Sigma, St. Louis, MO, USA), and blocked with GS (3%) for 60 min. Brain sections were then incubated overnight at 4°C with primary antibodies specific for tyrosine hydroxylase (TH) (Cell Signaling Tech.). Afterwards, brain sections were incubated for 1 h at room temperature with secondary antibodies conjugated with fluorescein isothiocyanate (Millipore Corporation, Billerica, MA, USA). Nuclei were labeled with 4′,6-diamidino-2-phenylindole (1 mg/mL) for 10 min at room temperature. Brain sections were mounted in glycerol and visualized by a fluorescence confocal microscope (FluoView, Olympus, Tokyo, Japan). TH-positive cells of three sections from each rat were counted.

Molecular docking and predicted partition coefficient

The X-ray structure of MEK1 as the receptor structure was taken from RCSB Protein Data Bank (PDB ID: 7JUS).[32] The three-dimensional (3D) structures and properties of ellagic acid as a potential ligand and selumetinib were obtained from PubChem (ellagic acid CID: 5281855; selumetinib CID: 10127622).[33] All docking runs were performed with the AutoDock Vina program.[34] In order to screen for the best binding sites, the ligand was docked against MEK1 with a large grid box $50 \times 50 \times 50$ Å^3 to include the ligand and protein for a global search. This approach allows a scoring function evaluation during the docking process so that as many conformations as possible can be obtained. The minimum scoring value indicates the most likely conformation. Thus, the grid box was centered on the ligand in its binding mode with a small box $30 \times 30 \times 30$ Å^3 for a local search. The results were represented with the best binding affinity. The logarithm octanol–water partition coefficient (log P) was calculated using the XLOGP3 3.0 tool.[34]

Statistics

Data were expressed as the mean ± SEM. The results of western blot assays were analyzed by one-way analysis of variance (one-way ANOVA) and *t*-test.

Results

Ellagic acid inhibited LPS-induced neuroinflammation via MEK–ERK pathway in BV-2 microglial cells

The antineuroinflammatory effects of ellagic acid were investigated using BV-2 cells treated with LPS (1 μg/mL) as an *in vitro* model of neuroinflammation. LPS significantly induced ERK phosphorylation 20 min after LPS incubation (Figure 1(A)). Incubation of ellagic acid (50, 100 μM) attenuated LPS-induced ERK phosphorylation in the treated BV-2 cells. In addition, ellagic acid concentration dependently inhibited LPS-induced elevation in TNF-α level 40 min (Figure 1(B)) and NO production 24 h after LPS incubation (Figure 1(C)). These *in vitro* data indicate that ellagic acid is capable of inhibiting MEK–ERK signaling pathway and LPS-induced neuroinflammation. Next, AutoDock Vina molecular docking

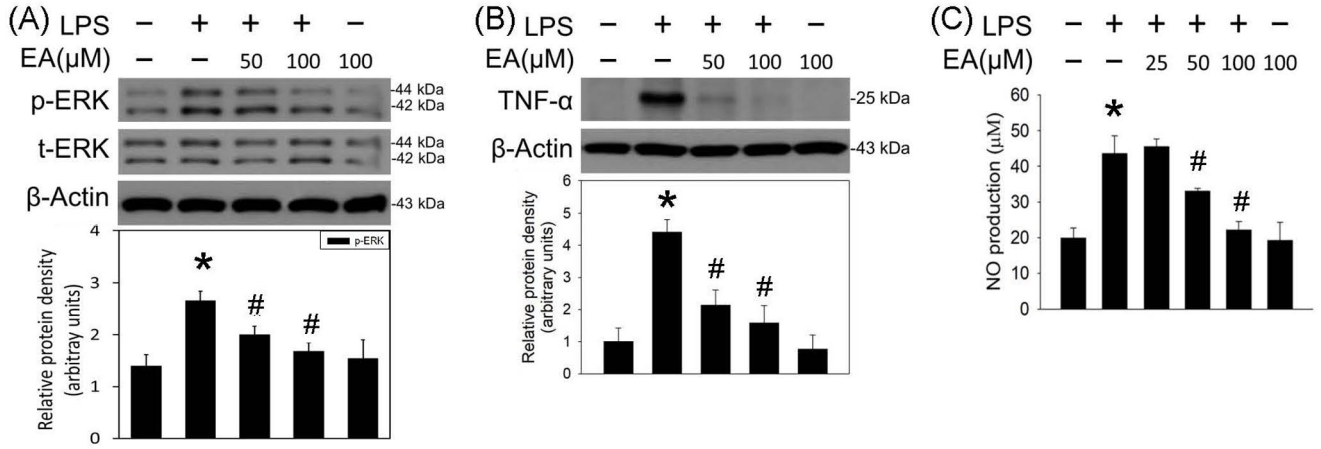

Figure 1. Ellagic acid inhibited LPS-induced ERK phosphorylation and proinflammatory cytokine in BV-2 cells. (A) and (B) BV-2 cells were treated with LPS (1 μg/mL) and ellagic acid (EA, 50, 100 μM) for 20 and 40 min, respectively. p-ERK in (A) and TNF-α in (B) were measured using the western blot assay. Graphs show statistical results from relative optical density of bands on the blots estimated by Image J software. (C) BV-2 cells were treated with LPS (1 μg/mL) and EA (25, 50, 100 μM) for 24 h. NO content was measured using the Griess reagents. Values are the mean ± SEM ($n = 3$/group). *$P < 0.05$ in the LPS group compared with the control group; #$P < 0.05$ in LPS plus EA groups compared with LPS group by one-way ANOVA and *t*-test.

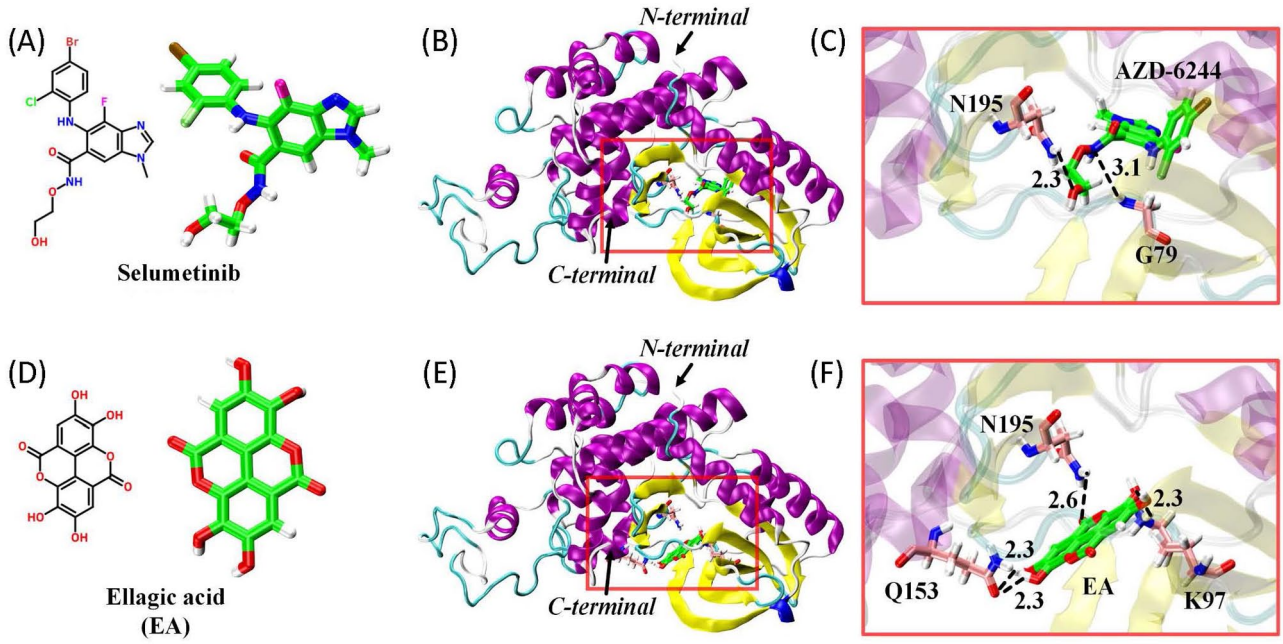

Figure 2. Binding models of ellagic acid and selumetinib with MEK1 protein (PDB code: 7JUS). (A) and (D): chemical structures of selumetinib and ellagic acid (EA). (B) and (E): spatial orientation of selumetinib and ellagic acid in MEK1 pocket. (C) and (F): hydrogen bonding formed between MEK1 and selumetinib as well as MEK1 and ellagic acid.

(Figure 2) was employed to investigate the interaction of ellagic acid and MEK1. Using selumetinib as a positive control (Figure 2(A) to (C)), ellagic acid (Figure 2(D)) binds to the catalytic site of MEK1 (Figure 2(E)). *In silico* data show that ellagic acid forms three hydrogen bonds with K97, Q153, and N195 (Figure 2(F)) while selumetinib forms two hydrogen bonds with N195 and G79 (Figure 2(C)). The calculated binding affinities of ellagic acid and selumetinib were, respectively, −8.7 and −8.1 kcal/mol, suggesting that the interaction between ellagic acid and MEK1 was better than that of selumetinib. However, the partition coefficient values for the membrane permeability of selumetinib and ellagic acid were 3.6 and 1.1, respectively.

Oral administration of ellagic acid inhibited LPS-induced ERK phosphorylation and neuroinflammation

An animal model of neuroinflammation was established by local infusion of LPS (4 μg/μL) in the SN of anesthetized rats. Intranigral infusion of LPS significantly increased the phosphorylated ERK levels in the LPS-infused SN 1 h after and maintained for 24 h (Figure 3(A)). Oral administration of ellagic acid (100 mg/kg) inhibited LPS-induced phosphorylation of ERK 3 h after intranigral infusion of LPS (Figure 3(B)). A four-day treatment of ellagic acid (100 mg/kg/daily) did not affect LPS-elevated ED-1 levels (a biomarker of activated microglia, Figure 3(C)) but attenuated LPS-induced

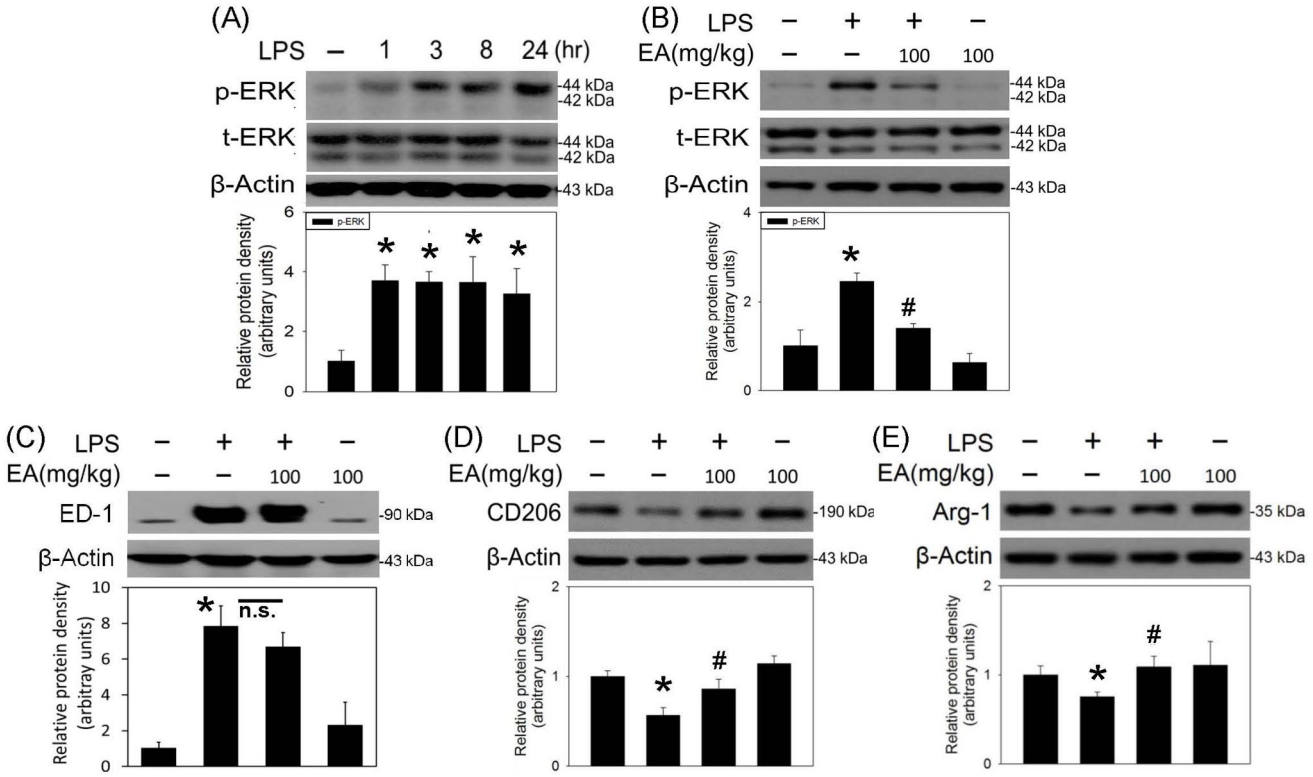

Figure 3. Ellagic acid inhibited LPS-induced ERK phosphorylation and modulated LPS-induced M1/M2 microglial polarization in rat SN. LPS (4 μg/μL) was locally infused in the SN of anesthetized rats. (A) A time-dependent effect of LPS on ERK phosphorylation was investigated in the SN. Phosphorylated ERK protein levels in SN were measured using the western blot assay. Values are the mean ± SEM ($n = 4$/group). (B) Oral administration of ellagic acid (EA) was pretreated 1 h prior to the intranigral infusion of LPS. Three hours after LPS infusion, p-ERK protein levels in SN were measured using the western blot assay. Values are the mean ± SEM ($n = 4$/group). (C) to (E) Oral administration of EA was performed 1 h prior to intranigral infusion of LPS and daily for four days. Protein levels of (C) ED-1, (D) CD206, and (E) arginase 1 (ARG-1) in SN were measured using the western blot assay. Graphs show statistical results from relative optical density of bands on the blots estimated by the Image J software. Values are the mean ± SEM ($n = 3$–4/group). *$P < 0.05$ in the LPS group compared with the control group; #$P < 0.05$ in LPS plus EA group compared with LPS group by one-way ANOVA and *t*-test.
n.s.: no significance.

reduction in CD206 and arginase 1 levels (biomarkers of M2 microglia, Figure 3(D) and (E)). These data indicate that ellagic acid is capable of increasing M2 microglia and decreasing M1 microglia in LPS-infused SN.

A seven-day treatment of ellagic acid inhibited LPS-induced oxidative responses and programmed cell death

Oxidative stress reportedly plays a critical role in neuroinflammation. In this study, the effect of ellagic acid was investigated by measuring HO-1 (a redox-regulated chaperone protein) and COX-2 (a proinflammatory enzyme and a regulator of polyunsaturated fatty acid peroxidation). The effect of oral administration of ellagic acid (100 mg/kg/daily) for seven days on the body weight was investigated. Compared with vehicle-treated rats, ellagic acid for seven days did not reduce body weight of the treated rats (Figure 4(A)). At the same time, ellagic acid significantly attenuated LPS-induced increases in HO-1 and COX-2 expression (Figure 4(B) and (C)) as well as α-synuclein trimers (51 kDa, Figure 4(D)) formation (a pathological biomarker of CNS neurodegeneration). These data indicate that ellagic acid is capable of reducing LPS-induced oxidative stress and protein aggregation. Furthermore, oral administration of ellagic acid significantly attenuated LPS-induced increases in cleaved caspase 3 (a biomarker of apoptosis) and receptor interacting serine/threonine kinase 3 (RIPK3, a biomarker of necroptosis) (Figure 5(A) and (B)). The immunofluorescent staining study demonstrated that the number of TH (a biomarker of dopaminergic neurons) positive cells was decreased in the LPS-infused SN. Systemic administration of ellagic acid prevented LPS-induced TH-positive cell loss (Figure 5(C) and (D)). These data indicate that ellagic acid is capable of inhibiting LPS-induced programmed cell death (apoptosis and necroptosis) and dopaminergic neuronal loss in the nigrostriatal dopaminergic system of rat brain.

Discussion

In this study, the cellular mechanisms underlying ellagic acid-induced neuroprotection were delineated as follows. First, both *in vitro* and *in vivo* data showed that ellagic acid is capable of inhibiting LPS-induced ERK phosphorylation. Molecular docking data show that ellagic acid may inhibit with MEK1.[32] Furthermore, oral administration of ellagic acid attenuated LPS-induced oxidative stress, protein aggregation, and programmed cell death in the infused SN. In addition, ellagic acid modulated microglial transition by preventing LPS-induced reduction in M2 microglia, suggesting

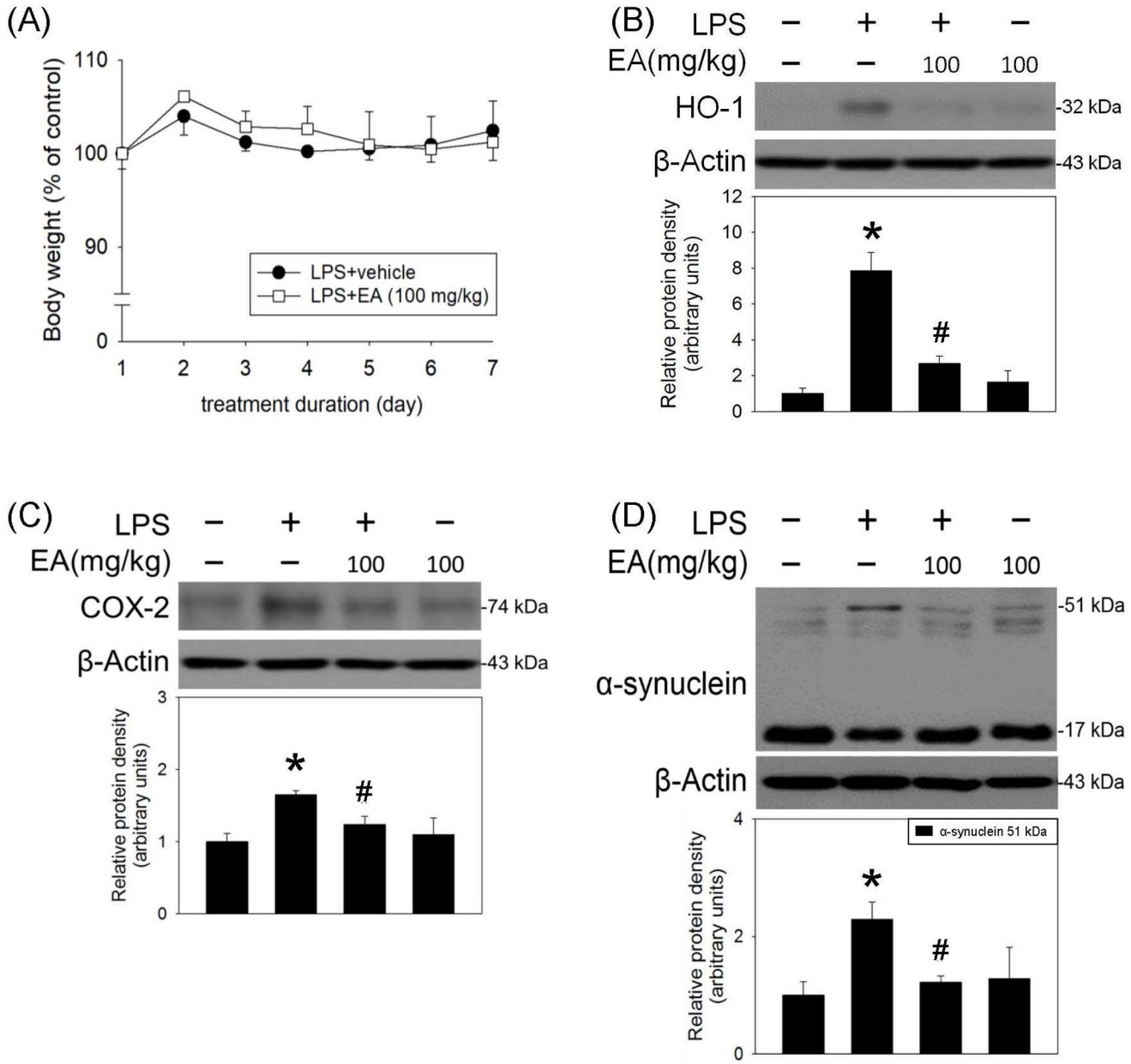

Figure 4. Ellagic acid attenuated LPS-induced oxidative stress and protein aggregation in rat SN. LPS (4 μg/μL) was locally infused in the SN of anesthetized rats. Oral administration of ellagic acid (EA) was performed 1 h prior to intranigral infusion of LPS and daily for seven days. (A) The effect of oral administration of EA for seven days on the body weight of rats. Values are the mean ± SEM ($n = 10$/group). Protein levels of (B) HO-1, (C) COX-2, and (D) α-synuclein aggregation in SN were measured using the western blot assay. Graphs show statistical results from relative optical density of bands on the blots estimated by the Image J software. Values are the mean ± SEM ($n = 3$–4/group). *$P < 0.05$ in the LPS group compared with the control group; #$P < 0.05$ in LPS plus EA group compared with LPS group by one-way ANOVA and *t*-test.

that targeting M2 microglial polarization is a novel neuroprotective mechanism. These data suggest that ellagic acid may exert its neuroprotective action via inhibiting MEK–ERK signaling and attenuating neuroinflammation in CNS.

Molecular-targeted therapies with definitive pharmacological mechanisms are developed for cancer treatment for more than two decades.[35] Recently, molecular target therapies for neuroprotection have attracted significant attention. For example, afatinib, an epidermal growth factor receptor-tyrosine kinase inhibitor for lung cancer, attenuated oxygen glucose deprivation-induced neuroinflammation in CTX-TNA2 astrocytes.[24] Dasatinib, an AKT/STAT 3 inhibitor for leukemia, suppressed LPS-induced neuroinflammation in microglia.[12] Moreover, selumetinib via inhibiting MEK–ERK signaling was found to attenuate neuroinflammation in BV-2 microglia[31] and neurotoxicity in primary neurons.[36] These studies support the significance of drug repurposing. Due to the adverse effects of targeted therapies, such as diarrhea and body weight loss, the need for potential therapies with the feature of molecular targeted therapies and less toxicities was urged for CNS neurodegenerative diseases. In addition to the western blot assay that showed ellagic acid-induced inhibition of ERK phosphorylation, *in silico* analysis was used to support the molecular mechanism of ellagic acid. Using selumetinib as a demonstration, we are the first to show that ellagic acid is capable of binding at the catalytic site of MEK1,[37] suggesting that ellagic acid may block MEK–ERK signaling as that of selumetinib.

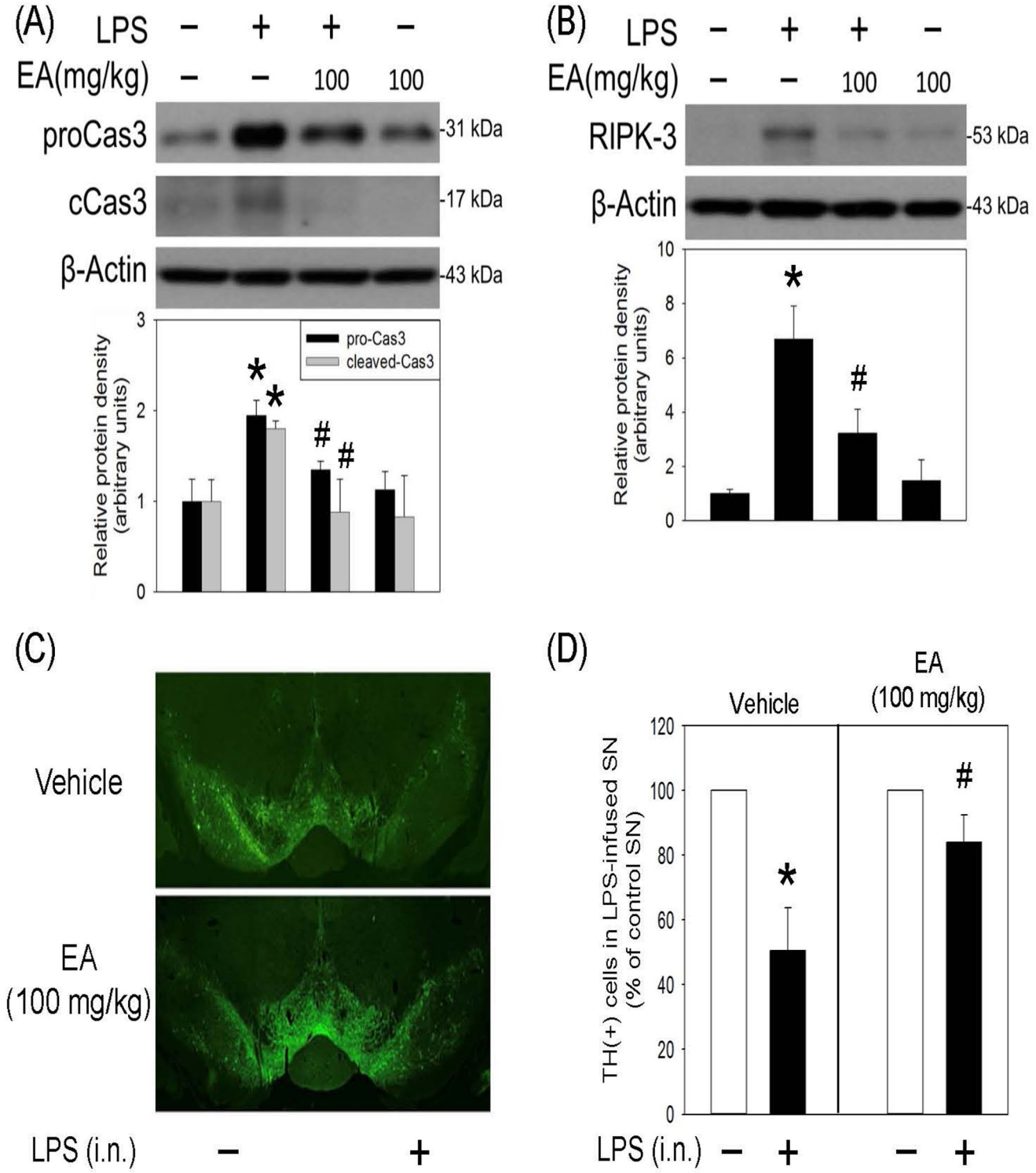

Figure 5. Ellagic acid inhibited LPS-induced programmed cell death in rat SN. LPS (4 μg/μL) was locally infused in the SN of anesthetized rats. Oral administration of ellagic acid (EA) was performed for seven days. Protein levels of (A) procaspase 3 and cleaved-caspase 3 as well as (B) RIPK3 in SN were measured by the western blot assay. Graphs show statistical results from relative optical density of bands on the blots estimated by the Image J software. Values are the mean ± SEM ($n = 3$/group). *$P < 0.05$ in the LPS group compared with the control group; #$P < 0.05$ in LPS plus EA group compared with LPS group by *t*-test. Similar results were observed in duplicates. (C) Representative confocal microscopic data showed TH-positive neurons in the SN of rat. (D) Statistical data showed TH-positive cells in SN receiving intranigral infusion (i.n.) of LPS were counted and expressed as % of that in the contralateral intact SN of the same rat. Values are the mean ± SEM ($n = 3$/group). *$P < 0.05$ in the LPS group compared with the control group; #$P < 0.05$ in LPS plus EA group compared with LPS group by one-way ANOVA and *t*-test.

The calculated affinity energy of ellagic acid was lower than that of selumetinib, indicating that ellagic acid has a better binding affinity to MEK1 than selumetinib. However, the logarithm octanol–water partition coefficient (log P)[38–40] of selumetinib is 3.6 and that of ellagic acid was 1.1, suggesting that ellagic acid is less lipophilic than selumetinib.

Many *in vivo* studies have reported the beneficial effects of ellagic acid from 1 to 200 mg/kg.[8,27,28,41] For CNS

neuroprotection, the optimal doses for ellagic acid were 50–100 mg/kg in 6-OHDA-induced neurodegeneration and neuroinflammation[27] as well as learning and memory deficits induced by Aβ and diazepam.[8] In this study, we chose 100 mg/kg ellagic acid that did not reduce the body weight of treated rats but significantly attenuated LPS-induced ERK phosphorylation and LPS-induced neuroinflammation and protein aggregation, indicating 100 mg/kg ellagic acid is effective and non-toxic. With this dosage, we found that ellagic acid is neuroprotective by mitigating LPS-induced active caspase 3 and RIPK3 as well as dopaminergic cell loss in the LPS-induced SN, indicating that ellagic acid is capable of inhibiting programmed cell death, that is, apoptosis and necroptosis.

Oxidative stress, protein aggregation, and cell death form a vicious cycle of CNS neurodegenerative diseases; neuroinflammation is reportedly the center of a pathological cycle. Neuroinflammation is clinically detected in the affected brain tissues of patients with CNS neurodegenerative diseases;[42] however, microglial dynamics is remained to be defined.[43] Using LPS, many studied have successfully mimicked neuroinflammation, such as increases in ED-1 or IBA-1, biomarkers of activated microglia. At the same time, LPS treatment has suggested to modulate M1/M2 transition.[20,44] During LPS-induced neuroinflammation, reduction in CD11 (an M1 biomarker) and elevation in arginase-1 (an M2 biomarker) has been identified.[44] However, Hong's study demonstrated that LPS increased iNOS and CD86 (two M1 biomarkers) but did not alter arginase-1.[45] In contrast, our studies found that LPS not only increased iNOS (M1 biomarker)[9] but decreased CD206 and arginase 1. In this study, we are the first to show that ellagic acid is capable of reversing LPS-induced reduction in CD206 and arginase 1, suggesting that ellagic acid may exert its neuroprotective action via shifting microglia polarization toward a more beneficial M2 microglia and less harmful M1 microglia. In this study, we employed *in vitro* and *in vivo* studies as well as *in silico* analysis to show the novel finding that MEK–ERK signaling pathway is involved in the ellagic acid–induced antineuroinflammation. Furthermore, ellagic acid is neuroprotective by inhibiting LPS-induced oxidative stress, protein aggregation, M2 microglial polarization, and programmed cell death of rat brain. Accordingly, M1/M2 microglial transition may be used as a druggable target for treating CNS neurodegenerative diseases.

AUTHORS' CONTRIBUTIONS

Y-LL carried out experiments and analyzed data. H-JH carried out the western blot assay. S-YS designed and carried out the molecular docking. Y-CL carried out the molecular docking. I-JL conceived the study. S-CC conceived and prepared the manuscript. AM-YL conceived and designed the study, analyzed data, and prepared the manuscript. All authors read and approved the final manuscript.

DECLARATION OF CONFLICTING INTERESTS

The author(s) declared no potential conflicts of interest with respect to the research, authorship, and/or publication of this article.

FUNDING

The author(s) disclosed receipt of the following financial support for the research, authorship, and/or publication of this article: This work was supported by program project grants from the MOST107-2320-B-010-019-MY3 and MOST 110-2320-B-A49A-509-MY3, and VGHTPE V109C-079.

ORCID IDS

Yu-Cheng Liu https://orcid.org/0000-0003-4669-2586

Anya Maan-Yuh Lin https://orcid.org/0000-0002-6203-5183

REFERENCES

1. Tejera D, Heneka MT. Microglia in neurodegenerative disorders. *Methods Mol Biol* 2019;**2034**:57–67
2. Khatri N, Thakur M, Pareek V, Kumar S, Sharma S, Datusalia AK. Oxidative stress: major threat in traumatic brain injury. *CNS Neurol Disord Drug Targets* 2018;**17**:689–95
3. Gomez-Nicola D, Boche D. Post-mortem analysis of neuroinflammatory changes in human Alzheimer's disease. *Alzheimers Res Ther* 2015;**7**:42
4. Sasaki A. Microglia and brain macrophages: an update. *Neuropathology* 2017;**37**:452–64
5. Lin AM, Wu LY, Hung KC, Huang HJ, Lei YP, Lu WC, Hwang LS. Neuroprotective effects of longan (*Dimocarpus longan* Lour.) flower water extract on MPP^+-induced neurotoxicity in rat brain. *J Agric Food Chem* 2012;**60**:9188–94
6. Hu X, Zhang D, Pang H, Caudle WM, Li Y, Gao H, Liu Y, Qian L, Wilson B, Di Monte DA, Ali SF, Zhang J, Block ML, Hong JS. Macrophage antigen complex-1 mediates reactive microgliosis and progressive dopaminergic neurodegeneration in the MPTP model of Parkinson's disease. *J Immunol* 2008;**181**:7194–204
7. Zhao WZ, Wang HT, Huang HJ, Lo YL, Lin AM. Neuroprotective effects of baicalein on acrolein-induced neurotoxicity in the nigrostriatal dopaminergic system of rat brain. *Mol Neurobiol* 2018;**55**:130–7
8. Kiasalari Z, Heydarifard R, Khalili M, Afshin-Majd S, Baluchnejadmojarad T, Zahedi E, Sanaierad A, Roghani M. Ellagic acid ameliorates learning and memory deficits in a rat model of Alzheimer's disease: an exploration of underlying mechanisms. *Psychopharmacology* 2017;**234**:1841–52
9. Liu YL, Hsu CC, Huang HJ, Chang CJ, Sun SH, Lin AM. Gallic acid attenuated LPS-induced neuroinflammation: protein aggregation and necroptosis. *Mol Neurobiol* 2020;**57**:96–104
10. Wang Y, Wu Y, Liang C, Tan R, Tan L, Tan R. Pharmacodynamic effect of ellagic acid on ameliorating cerebral ischemia/reperfusion injury. *Pharmacology* 2019;**104**:320–31
11. Spangenberg EE, Green KN. Inflammation in Alzheimer's disease: lessons learned from microglia-depletion models. *Brain Behav Immun* 2017;**61**:1–11
12. Ryu KY, Lee HJ, Woo H, Kang RJ, Han KM, Park HH, Lee SM, Lee JY, Jeong YJ, Nam HW, Nam Y, Hoe HS. Dasatinib regulates LPS-induced microglial and astrocytic neuroinflammatory responses by inhibiting AKT/STAT3 signaling. *J Neuroinflammation* 2019;**16**:190
13. Kaushik DK, Basu A. A friend in need may not be a friend indeed: role of microglia in neurodegenerative diseases. *CNS Neurol Disord Drug Targets* 2013;**12**:726–40
14. Loane DJ, Kumar A. Microglia in the TBI brain: the good, the bad, and the dysregulated. *Exp Neurol* 2016;**275**:316–27
15. Tang Y, Le W. Differential roles of M1 and M2 microglia in neurodegenerative diseases. *Mol Neurobiol* 2016;**53**:1181–94
16. Chhor V, Le Charpentier T, Lebon S, Oré MV, Celador IL, Josserand J, Degos V, Jacotot E, Hagberg H, Sävman K, Mallard C, Gressens P, Fleiss B. Characterization of phenotype markers and neuronotoxic potential of polarised primary microglia in vitro. *Brain Behav Immun* 2013;**32**:70–85

17. Batista CRA, Gomes GF, Candelario-Jalil E, Fiebich BL, de Oliveira ACP. Lipopolysaccharide-induced neuroinflammation as a bridge to understand neurodegeneration. *Int J Mol Sci* 2019;**20**:2293
18. Chang RC, Chen W, Hudson P, Wilson B, Han DS, Hong JS. Neurons reduce glial responses to lipopolysaccharide (LPS) and prevent injury of microglial cells from over-activation by LPS. *J Neurochem* 2001;**76**:1042–9
19. Hoogland IC, Houbolt C, van Westerloo DJ, van Gool WA, van de Beek D. Systemic inflammation and microglial activation: systematic review of animal experiments. *J Neuroinflammation* 2015;**12**:114
20. Li J, Shui X, Sun R, Wan L, Zhang B, Xiao B, Luo Z. Microglial phenotypic transition: signaling pathways and influencing modulators involved in regulation in central nervous system diseases. *Front Cell Neurosci* 2021;**15**:736310
21. Hernandez Baltazar D, Nadella R, Barrientos Bonilla A, Flores Martínez Y, Olguín A, Heman Bozadas P, Rovirosa Hernández M, Cibrián Llanderal I. Does lipopolysaccharide-based neuroinflammation induce microglia polarization? *Folia Neuropathol* 2020;**58**:113–22
22. Kalkman HO, Feuerbach D. Antidepressant therapies inhibit inflammation and microglial M1-polarization. *Pharmacol Ther* 2016;**163**: 82–93
23. Xia CY, Zhang S, Gao Y, Wang ZZ, Chen NH. Selective modulation of microglia polarization to M2 phenotype for stroke treatment. *Int Immunopharmacol* 2015;**25**:377–82
24. Chen YJ, Hsu CC, Shiao YJ, Wang HT, Lo YL, Lin AMY. Anti-inflammatory effect of afatinib (an EGFR-TKI) on OGD-induced neuroinflammation. *Sci Rep* 2019;**9**:2516
25. De Oliveira MR. The effects of ellagic acid upon brain cells: a mechanistic view and future directions. *Neurochem Res* 2016;**41**:1219–28
26. Ríos JL, Giner RM, Marín M, Recio MC. A pharmacological update of ellagic acid. *Planta Med* 2018;**84**:1068–93
27. Baluchnejadmojarad T, Rabiee N, Zabihnejad S, Roghani M. Ellagic acid exerts protective effect in intrastriatal 6-hydroxydopamine rat model of Parkinson's disease: possible involvement of ERβ/Nrf2/HO-1 signaling. *Brain Res* 2017;**1662**:23–30
28. Farbood Y, Sarkaki A, Dolatshahi M, Taqhi Mansouri SM, Khodadadi A. Ellagic acid protects the brain against 6-hydroxydopamine induced neuroinflammation in a rat model of Parkinson's disease. *Basic Clin Neurosci* 2015;**6**:83–9
29. Takeuchi O, Akira S. Toll-like receptors; their physiological role and signal transduction system. *Int Immunopharmacol* 2001;**1**:625–35
30. Fan H, Li D, Guan X, Yang Y, Yan J, Shi J, Ma R, Shu Q. MsrA suppresses inflammatory activation of microglia and oxidative stress to prevent demyelination via inhibition of the NOX2-MAPKs/NF-kappaB signaling pathway. *Drug Des Devel Ther* 2020;**14**:1377–89
31. Ho WC, Hsu CC, Huang HJ, Wang HT, Lin AM. Anti-inflammatory effect of AZD6244 on acrolein-induced neuroinflammation. *Mol Neurobiol* 2020;**57**:88–95
32. Khan ZM, Real AM, Marsiglia WM, Chow A, Duffy ME, Yerabolu JR, Scopton AP, Dar AC. Structural basis for the action of the drug trametinib at KSR-bound MEK. *Nature* 2020;**888**:509–14
33. Kim S, Chen J, Cheng T, Gindulyte A, He J, He S, Li Q, Shoemaker BA, Thiessen PA, Yu B, Zaslavsky L, Zhang J, Bolton EE. PubChem 2019 update: improved access to chemical data. *Nucleic Acids Res* 2019;**47**:D1102–9
34. Trott O, Olson AJ. AutoDock Vina: improving the speed and accuracy of docking with a new scoring function, efficient optimization, and multithreading. *J Comput Chem* 2010;**31**:455–61
35. Hou J, He Z, Liu T, Chen D, Wang B, Wen Q, Zheng X. Evolution of molecular targeted cancer therapy: mechanisms of drug resistance and novel opportunities identified by CRISPR-Cas9 screening. *Front Oncol* 2022;**12**:755053
36. Huang HJ, Wang HT, Yeh TY, Lin BW, Shiao YJ, Lo YL, Lin AMY. Neuroprotective effect of selumetinib on acrolein-induced neurotoxicity. *Sci Rep* 2021;**11**:12497
37. Fischmann TO, Smith CK, Mayhood TW, Myers JE, Reichert P, Mannarino A, Carr D, Zhu H, Wong J, Yang RS, Le HV, Madison VS. Crystal structures of MEK1 binary and ternary complexes with nucleotides and inhibitors. *Biochemistry* 2009;**48**:2661–74
38. Manners CN, Payling DW, Smith DA. Distribution coefficient, a convenient term for the relation of predictable physico-chemical properties to metabolic processes. *Xenobiotica* 1988;**18**:331–50
39. Lipinski CA. Drug-like properties and the causes of poor solubility and poor permeability. *J Pharmacol Toxicol Methods* 2000;**44**:235–49
40. Comer J, Tam K. Lipophilicity profiles: theory and measurement. Pharmacokinetic optimization in drug research. Weinheim: Wiley-VCH, 2001, pp.275–304
41. Lee JH, Won JH, Choi JM, Cha HH, Jang YJ, Park S, Kim HG, Kim HC, Kim DK. Protective effect of ellagic acid on concanavalin A-induced hepatitis via toll-like receptor and mitogen-activated protein kinase/nuclear factor κB signaling pathways. *J Agric Food Chem* 2014;**62**:10110–7
42. Walker DG, Lue LF. Immune phenotypes of microglia in human neurodegenerative disease: challenges to detecting microglial polarization in human brains. *Alzheimers Res Ther* 2015;**7**:56
43. Javanmehr N, Saleki K, Alijanizadeh P, Rezaei N. Microglia dynamics in aging-related neurobehavioral and neuroinflammatory diseases. *J Neuroinflammation* 2022;**19**:273
44. Liu L, Fang L, Duan B, Wang Y, Cui Z, Yang L, Wu D. Multi-hit white matter injury-induced cerebral palsy model established by perinatal lipopolysaccharide injection. *Front Pediatr* 2022;**10**:867410
45. Hong J, Yoon D, Nam Y, Seo D, Kim JH, Kim MS, Lee TY, Kim KS, Ko PW, Lee HW, Suk K, Kim SR. Lipopolysaccharide administration for a mouse model of cerebellar ataxia with neuroinflammation. *Sci Rep* 2020;**10**:13337

(Received February 11, 2023, Accepted March 20, 2023)